

Electrical coupling and innexin expression in the stomatogastric ganglion of the crab *Cancer borealis*

Sonal Shruti, David J. Schulz, Kawasi M. Lett and Eve Marder

J Neurophysiol 112:2946-2958, 2014. First published 10 September 2014; doi:10.1152/jn.00536.2014

You might find this additional info useful...

This article cites 84 articles, 39 of which can be accessed free at:

</content/112/11/2946.full.html#ref-list-1>

Updated information and services including high resolution figures, can be found at:

</content/112/11/2946.full.html>

Additional material and information about *Journal of Neurophysiology* can be found at:

<http://www.the-aps.org/publications/jn>

This information is current as of February 4, 2015.

Electrical coupling and innexin expression in the stomatogastric ganglion of the crab *Cancer borealis*

Sonal Shruti,¹ David J. Schulz,² Kawasi M. Lett,² and Eve Marder¹

¹Volen Center and Biology Department, Brandeis University, Waltham, Massachusetts; and ²Division of Biological Sciences, University of Missouri at Columbia, Columbia, Missouri

Submitted 21 July 2014; accepted in final form 6 September 2014

Shruti S, Schulz DJ, Lett KM, Marder E. Electrical coupling and innexin expression in the stomatogastric ganglion of the crab *Cancer borealis*. *J Neurophysiol* 112: 2946–2958, 2014. First published September 10, 2014; doi:10.1152/jn.00536.2014.—Gap junctions are intercellular channels that allow for the movement of small molecules and ions between the cytoplasm of adjacent cells and form electrical synapses between neurons. In invertebrates, the gap junction proteins are coded for by the innexin family of genes. The stomatogastric ganglion (STG) in the crab *Cancer borealis* contains a small number of identified and electrically coupled neurons. We identified Innexin 1 (*Inx1*), Innexin 2 (*Inx2*), Innexin 3 (*Inx3*), Innexin 4 (*Inx4*), Innexin 5 (*Inx5*), and Innexin 6 (*Inx6*) members of the *C. borealis* innexin family. We also identified six members of the innexin family from the lobster *Homarus americanus* transcriptome. These innexins show significant sequence similarity to other arthropod innexins. Using *in situ* hybridization and reverse transcriptase-quantitative PCR (RT-qPCR), we determined that all the cells in the crab STG express multiple innexin genes. Electrophysiological recordings of coupling coefficients between identified pairs of pyloric dilator (PD) cells and PD-lateral posterior gastric (LPG) neurons show that the PD-PD electrical synapse is nonrectifying while the PD-LPG synapse is apparently strongly rectifying.

gap junctions; electrical synapses; crustaceans; phylogeny; reverse transcriptase-quantitative PCR

GAP JUNCTIONS ARE CLUSTERS of intercellular channels that connect the cytoplasm of two adjacent cells and allow for passage of small molecules between cells. Gap junction-mediated electrical synapses are widely distributed in both vertebrate and invertebrate nervous systems (Anava et al. 2009; Blagburn et al. 1999; Deans et al. 2001; Devor and Yarom 2002; Dykes and Macagno 2006; Landisman et al. 2002; Pereda et al. 2013; Rash et al. 1996; Sasaki et al. 2013; Starich et al. 2009; Weaver et al. 2010; White et al. 1986; reviewed in Connors and Long 2004; Pereda et al. 2013). In addition to electrical synapses between cell bodies, gap junctions are also frequently found in dendrites and at nerve terminals (Furshpan and Potter 1959; Nagy et al. 2013; Pereda et al. 2013). Although many of these electrical synapses promote synchronization of networks (Beierlein et al. 2000; Lewis and Rinzel 2000; Pfeuty et al. 2003; Traub et al. 2001), electrical synapses can cause network desynchronization in the presence of sparse excitatory inputs (Vervaeke et al. 2010), and electrical coupling has long been known to be consistent with alternations in activity patterns (Bem et al. 2005; Sherman and Rinzel 1992) and developmental changes in network properties (Ducret et al. 2007). There is growing evidence to suggest that electrical synapses are plastic

and their regulation can help a neuronal network to respond to changes in inputs (reviewed in O'Brien 2014).

Gap junctions are formed by the close apposition of a hexamer of gap junction proteins in adjacent cells (Caspar et al. 1977). These proteins belong to the connexin family in vertebrates (Beyer et al. 1987; Cruciani and Mikalsen 2007). In invertebrates, gap junctions are formed by members of the innexin protein family (Phelan et al. 1998). Although connexins and innexins are not evolutionarily related (Hua et al. 2003), innexins are homologous to the vertebrate pannexin proteins known to primarily form hemichannels connecting intracellular and extracellular space (Bao et al. 2004; Panchin et al. 2000). Each species has a number of gap junction proteins whose distribution might vary based on cell type and developmental stage (Bauer et al. 2005; Ducret et al. 2006; Kandarian et al. 2012; Nadarajah et al. 1997; Nagy et al. 2004; Starich et al. 1996). For example, there are 21 innexins in the medicinal leech (Kandarian et al. 2012), 25 innexins in *Caenorhabditis elegans* (Starich et al. 2001), and 8 different innexins in *Drosophila*, in addition to multiple splice variants (Curtin et al. 1999; Stebbings et al. 2002). Within crustaceans, two innexin genes had been previously found in the lobster stomatogastric nervous system (Ducret et al. 2006). This diversity in the number of gap junction proteins is important because the molecular identity of the participating innexins or connexins at a particular electrical synapse determines the properties of the synapse (Pereda et al. 2013; Phelan et al. 2008).

Electrical synapses are not simple bidirectional channels that allow for free flow of small molecules in both directions. Some synapses can be rectifying; positive current flows preferentially in one direction through the gap junction channel. In fact, rectifying properties of electrical synapses were observed more than fifty years ago in the very first experiments that identified electrical synapses (Furshpan and Potter 1959) and have since been found in various preparations (Auerbach and Bennett 1969; Rela and Szczupak 2007; Spray et al. 1979; reviewed in Marder 2009). Gap junctions can be either homotypic or heterotypic (Bittman et al. 2002), and previous work in cell cultures, goldfish Mauthner cells, and *Drosophila* suggest that rectifying electrical synapses are associated with heterotypic gap junctions (Bukauskas et al. 2002; Phelan et al. 2008; Rash et al. 2013; Wu et al. 2011). Rectification can significantly alter the network's sensitivity to change in synaptic strength (Gutierrez and Marder 2013), while rectifying electrical synapses can themselves be modulated by changes in postsynaptic membrane potential (Edwards et al. 1991).

Address for reprint requests and other correspondence: S. Shruti, Volen Center and Biology Dept., Brandeis Univ., Waltham, MA 02454.

Given the important role of electrical synapses in the function of neuronal circuits, and the large variability in the properties of these synapses, it is important to understand the relationship between the gap junction proteins expressed in a particular cell and the properties of the electrical synapses formed by that cell. The stomatogastric ganglion (STG) in crustaceans provides a platform for simultaneously studying the molecular and physiological properties of gap junctions. The STG consists of a small number of neurons that can be identified electrophysiologically and isolated for molecular biology (Baro et al. 1994, 1996; Schulz et al. 2006, 2007). Electrical synapses between multiple STG cell pairs are well documented and play a significant role in generating and regulating the rhythmic oscillatory output of the STG (Hooper and Marder 1987; Kepler et al. 1990; Soto-Trevino et al. 2005). The strength of these synapses may also contribute to the ability of certain cells to switch between the pyloric and gastric rhythms produced by this ganglion (Gutierrez et al. 2013; Weimann and Marder 1994). Additionally, similar to other networks, there is evidence for neuromodulation-induced plasticity in these electrical synapses (Johnson et al. 1993a, 1993b, 1994). Despite the importance of electrical synapses in this circuit, there has been little investigation into the molecular basis of the physiological properties of these synapses. We investigated rectifying and nonrectifying gap junctions within the STG and took advantage of our ability to perform electrophysiology and reverse transcriptase-quantitative PCR (RT-qPCR) on the same identified cells to see whether there is any correlation between these properties.

METHODS

Cloning and sequencing. We cloned and sequenced the cDNA for three innexin genes in the crab *Cancer borealis*: Innixin 1 (*Inx1*), Innixin 2 (*Inx2*), and Innixin 3 (*Inx3*). We isolated total RNA from crab tissue (mix of brain and STG) with TRIzol reagent (Invitrogen, 15596-026) and prepared cDNA with the SuperScript III First-Strand Synthesis System (Invitrogen, 18080-051). For *Inx2* and *Inx3*, PCR was performed on this cDNA with degenerate primers designed with the CODEHOP program (at <http://blocks.fhcrc.org/codehop.html>) based on conserved protein sequence alignments from *Drosophila melanogaster*, *Aedes egyptii*, *Hirudo medicinalis*, and *Homarus gammarus* innexins. The sequence of the degenerate primer pair is as follows: forward primer 5'-GAGGACGAGATCAAGTACCACA-CATAYTAYCARTGG-3'; reverse primer 5'-GGTCATGAAGGT-CAGGAAGACGWRCARAAACC-3'. PCR products of appropriate length were cloned into pCR 2.1 TOPO cloning vector (Invitrogen, 45-0641) and verified by sequencing (Genewiz). For *Inx1*, degenerate primers were designed by hand based on conserved protein sequence alignments from *D. melanogaster*, *Anopheles gambiae*, *Bombyx mori*, and *Schistocerca gregaria* innexins. The sequence of the degenerate primer pair is as follows: forward primer 5'-TAYTAYCARTGGGT-NTGYTTY-3'; reverse primer 5'-CCARAACCANARRAANA-CRTA-3'. PCR products of appropriate length were cloned into pGEMT-easy cloning vector (Promega) and verified by sequencing (University of Missouri DNA core). Full-length sequences for all three innexins were obtained by performing 5' and 3' RLM-RACE with the First Choice RLM-RACE kit (Ambion, AM1700).

C. borealis Innixin 4 (*Inx4*), Innixin 5 (*Inx5*), and Innixin 6 (*Inx6*) and *Homarus americanus* Innixin 1 (*Inx1*), Innixin 2 (*Inx2*), Innixin 3 (*Inx3*), Innixin 4 (*Inx4*), Innixin 6 (*Inx6*), and Innixin 7 (*Inx7*) coding sequences were identified via a translated nucleotide query of a nonredundant protein sequence database (GenBank) via BLASTX from custom-generated transcriptome sequence assemblies (Genewiz,

South Plainfield, NJ) derived from mixed nervous system tissue of *C. borealis* and *H. americanus*. The open reading frame was generated based on sequence similarity after identification of ATG start sequence and stop codon corresponding to orthologous sequences via *in silico* translation from all six possible reading frames via the SIXFRAME algorithm.

In situ hybridization. In situ hybridization was performed with digoxigenin (DIG)-labeled locked nucleic acid (LNA) probes. The probes were designed with Exiqon probe designing software and synthesized by Exiqon. The probe sequences were as follows: *Inx1* 5'-/5DigN/AGACTTCCTCTTCCTTATGCA-3'; *Inx3* 5'-/5DigN/ AGCCAGAACCGAGATGAAGATGA-3'. Cells in the STG were electrophysiologically identified, and their location was marked on a photograph of the ganglion. The STG was immediately fixed overnight in 4% paraformaldehyde (PFA) in phosphate-buffered saline (PBS), washed thoroughly in 1× PBS (Fisher Scientific, BP399), and placed in 1× PBS-0.1% Tween 20 (PTW; Fisher Scientific, BP337) for 10 min. The ganglion was dehydrated in a PTW:methanol dehydration series and stored in 100% methanol at -20°C until use. The preparations were rehydrated in a PTW:methanol hydration series and kept in PTW for 10 min, followed by 0.3% Triton X-100-PBS for 10 min and PTW for 5 min. This was followed by 2× glycine (2 mg/ml; Sigma Aldrich, G7126)-PTW and 3× PTW washes. The ganglia were then washed twice in TEA HCl (pH 8.0; Sigma Aldrich, 90279) and placed in 0.5% acetic anhydride-TEA HCl for 10 min with stirring, followed by further PTW washes. The samples were then placed in hybridization buffer [50% formamide (Sigma Aldrich, F7508), 5 mM EDTA (GIBCO, 15575), 5× SSC (Invitrogen, 15557-044), 1× Denhardt solution (USB, 70468), 0.1% Tween 20, 0.5 mg/ml yeast tRNA (GIBCO, 15401)] overnight at -20°C and then at 55°C for 6 h. For hybridization, DIG-LNA probes were applied to the samples in hybridization buffer (40 nM) and left overnight at 55°C. Posthybridization washes were done with 50% formamide-5× SSC-1% SDS (USB, 75832) at 65°C followed by 50% formamide-2× SSC-1% SDS (65°C) for 30 min each. This was followed by two washes in 0.2× SSC at 60°C for 30 min each and four washes with 1× PBS-0.1% Triton X-100-2 mg/ml BSA (PBT). The samples were then blocked in 10% normal goat serum in PBT at 4°C for 60 min, and alkaline phosphatase-conjugated anti DIG antibody (Roche Applied Science) was applied at 1:2,500 in 1% goat serum in PBT at 4°C overnight. After antibody incubation, the samples were washed in PBT (5 times, 20 min each) and detection buffer [100 mM NaCl, 50 mM MgCl₂, 0.1% Tween 20, 1 mM levamisol (Sigma Aldrich, L9756), 100 mM Tris-HCl, pH 9.5] twice for 5 min each. Each ganglion was then placed in 1 ml of detection buffer to which 20 μl of NBT-BCIP solution was added (DIG Nucleic Acid Detection kit, Roche Applied Science, 11175041910) and incubated at room temperature until color developed. Staining was stopped by placing in 1× PBS, and the stain was fixed in 4% PFA for 15 min at room temperature. The stained ganglia were dehydrated through a quick (2 min at each step) PBS:methanol dehydration series and kept in 100% ethanol. The samples were cleared in methyl salicylate and mounted in Permount (Fisher Scientific, SP15-500). The number of stained cells was counted and data analyzed in Microsoft Excel. All data presented are means ± SD.

RT-PCR. To screen for innixin expression in different tissues of the crab, we collected muscle tissue from skeletal muscle as well as cardiac muscle fibers and nervous system tissue from four different sources: brain, whole STG, commissural ganglia (CoG), and esophageal ganglia (OG). CoG and OG are ganglia within the stomatogastric nervous system that provide descending modulatory input to the STG (Blitz et al. 1999; Dickinson and Marder 1989). Total RNA was isolated from these tissues with TRIzol per the protocol provided by the manufacturer (Invitrogen). cDNA to be used as a template in subsequent PCR reactions was generated from oligo(dT)-primed total RNA that was reverse transcribed with SuperScript III reverse transcriptase (Invitrogen).

To perform single-cell RT-PCR, STG cells were electrophysiologically identified and their location was marked on a photograph of the STG. A Vaseline well was built around the STG, and the ganglion was treated with 10 mg/ml protease (Sigma Aldrich, P6141) in *C. borealis* saline (see *Electrophysiology*) for 10–15 min. Protease was washed out with saline when the cells started to become loose, and the well was filled with 70% ethylene glycol-30% saline at −20°C. The area surrounding the well was filled with distilled water, and the dish was frozen at −20°C for at least 1 h. The identified cell somata were then separated and picked individually by handheld forceps and placed in lysis buffer (400 µl, ZR RNA MicroPrep, Zymo Research) and frozen at −80°C until RNA extraction. RNA extraction was performed with the ZR RNA MicroPrep kit (Zymo Research, R1061), and cDNA was prepared with the SuperScript III First-Strand Synthesis System (Invitrogen, 18080-051) with a mix of oligo(dT) primers and random hexamers.

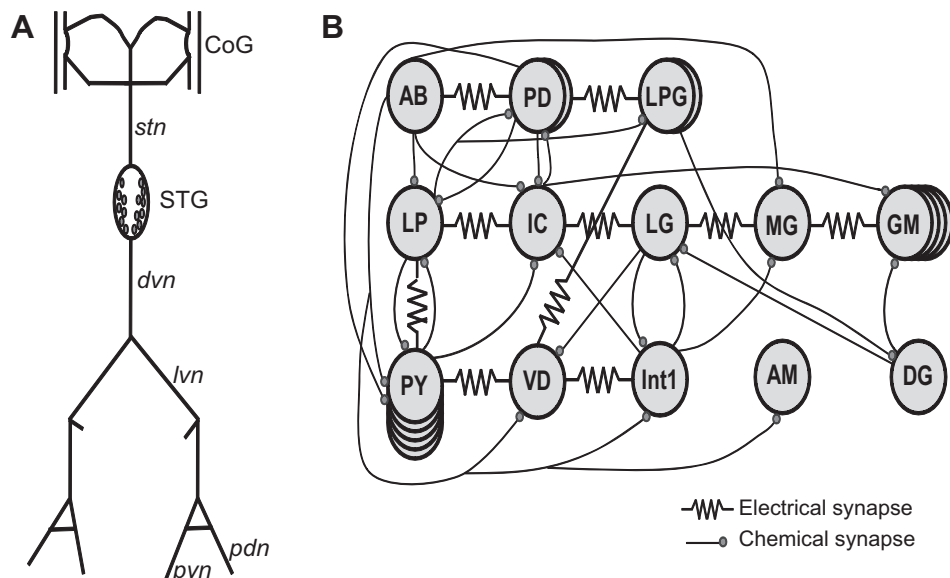
For qualitative RT-PCR screening of *Inx1–6* expression, PCR was performed with template from tissues and single-cell cDNA with GoTaq enzyme (Promega) with the following cycling parameters: initial denaturing at 95°C for 30 s followed by 95°C for 15 s, 59°C for 15 s, and 72°C for 30 s, for a total of 40 cycles and a final extension at 72°C for 2 min. Gene-specific primers were used at a final concentration of 500 nM each. The primer sequences are as follows (F, forward; R, reverse): *Inx1F* 5'-GTGAAGGACTCAACCCAGGA-3', *Inx1R* 5'-ACGGACCAAACCTTGTGGAAG-3'; *Inx2F* 5'-CGAA-CTGCTCAATTCTGTGA-3', *Inx2R* 5'-AGCCTACACCAGA-CACCAC-3'; *Inx3F* 5'-GAAGTTGGGACCATCAGGAA-3', *Inx3R* 5'-CCAAAGGTGGTAGATCAGGA-3'; *Inx4F* 5'-CTTAGCGGA-CAACCTCAAGC-3', *Inx4R* 5'-GGCAGGATACAGAGCGAGTC-3'; *Inx5F* 5'-GACAACACGCCTTCAGGTT-3', *Inx5R* 5'-CCTCT-CGTGATGCTTGGATT-3'; *Inx6F* 5'-CCAAACTGGTCGCT-TAGCTC-3', *Inx6R* 5'-CCGACGTTCCGTACATACCT-3'. Band sizes produced by each of the primer sets are as follows: *Inx1* = 312 bp, *Inx2* = 309 bp, *Inx3* = 280 bp, *Inx4* = 282 bp, *Inx5* = 252 bp, *Inx6* = 298 bp.

cDNA for quantitative PCR was further purified by ethanol precipitation and resuspended in nuclease-free water. The cDNA was used to set up a 30-µl PCR reaction in 1× RT2 SYBR Green Fluor PCR Master Mix (Qiagen, 330511). This reaction was divided into three technical replicates (10 µl each), and PCR was performed in a RotorGene 3000 thermocycler (Corbett Research). The PCR was run with the following parameters: 95°C for 3 min followed by 40 cycles of 95°C for 20 s, 58°C for 20 s, 72°C for 20 s. Standard curves were generated with known amounts of plasmid DNA containing the target

sequence, and these curves were used to calculate the mRNA copy number for single-cell cDNA. Data were analyzed with Rotor-Gene Q software and Microsoft Excel. All values presented are means ± SD. The primer pairs used for qPCR were designed with Primer3 software. The primers are as follows: *Inx1F* 5'-GCATATTGGATGCA-CAATG-3', *Inx1R* 5'-CTCCGAGGAAAGTGTCAACC-3'; *Inx2F* 5'-GCAAGGCTATGGTGGAT-3', *Inx2R* 5'-AAATCTGG-CAATGACGTT-3'; *Inx3F* 5'-ATCTCATCGCGAAGAAGTGC-3', *Inx3R* 5'-TTGAGGAACCTCCCCATAAACCC-3'. In crustacean motor neurons at the single-cell level, comparable patterns of mRNA levels can be quantified equally well with and without normalization of real-time results to 18S rRNA (Tobin et al. 2009), and there is evidence that normalization can obscure differences in total transcript number at the single-cell level (Ransdell et al. 2010). Therefore we report the raw copy number per cell as the least-derived measure of innixin expression in STG neurons.

Electrophysiology. Adult *C. borealis* crabs were obtained from Commercial Lobster (Boston, MA) and maintained in artificial seawater. Crabs were anesthetized by keeping them on ice for 30 min. The STG was dissected out and pinned on a Sylgard-coated dish containing physiological *C. borealis* saline (in mM: 440 NaCl, 11 KCl, 13 CaCl₂, 26 MgCl₂, 12.4 Trizma base, 5.3 maleic acid, pH 7.4–7.5). The STG was desheathed, and Vaseline wells were placed on the lateral ventricular nerve, pyloric dialtor nerve, and pyloric nerves (Fig. 1A). Extracellular recordings from these nerves were made with stainless steel electrodes placed in the wells, and an amplifier (A-M Systems) was used to amplify and filter the signals. Intracellular recordings were obtained with glass microelectrodes (15–25 MΩ) filled with 600 mM K₂SO₄ and 20 mM KCl and an Axoclamp 2A amplifier (Axon Instruments). Neurons were identified with standard procedures for *C. borealis* (Hooper et al. 1986; Weimann et al. 1991). The preparations were continuously superfused with chilled (12–14°C) physiological saline throughout the recordings. Electrical coupling was measured in discontinuous current-clamp (DCC) mode by injecting 1-s-long current steps from −3 nA to +4 nA (0.5-nA change between successive steps) in one neuron and simultaneously recording membrane voltage change in the injected cell and cells coupled to it. All cells were maintained at around −55 mV membrane potential. Steady-state voltage change was measured as an average of five sweeps. Electrical coupling was measured in the presence of 0.1 µM tetrodotoxin (TTX). Change in membrane voltage in the injected cell after hyperpolarizing current injection was plotted against voltage change in the coupled cells. This graph was fit with a line, and the slope of the line was calculated to give the coupling coefficient. Data were

Fig. 1. Schematic overview of the stomatogastric nervous system (STNS) and circuitry of the stomatogastric ganglion (STG). A: diagram of the STNS showing positions of the STG, commissural ganglia (CoG), stomatogastric nerve (stn), dorsal ventricular nerve (dvn), lateral ventricular nerve (lvn), pyloric dilator nerve (pdn), and pyloric nerve (pyn). B: schematic of the STG circuit. AB, anterior burster; PD, pyloric dilator; LPG, lateral posterior gastric; LP, lateral pyloric; LG, lateral gastric; MG, medial gastric; GM, gastric mill; PY, pyloric constrictor; VD, ventral dilator; Int1, interneuron 1; DG, dorsal gastric; IC, inferior cardiac; AM, anterior median.



acquired with a Digidata 1440A acquisition board (Axon Instruments) and pCLAMP 10 and analyzed with Clampfit (Axon Instruments) and Origin software. All values presented are means \pm SD.

RESULTS

The STG (Fig. 1A) of the crab contains 26 or 27 identifiable neurons that make multiple electrical synapses within the circuit (Fig. 1B). In this study we attempt to characterize the molecular components of the electrical synapses in the crab STG. Two strategies resulted in identification of the putative innexin genes: 1) identification of innexin transcripts by RT-PCR from STG mRNA and 2) bioinformatic screening of transcriptomes made from *C. borealis* and *H. americanus* nervous system tissue, with subsequent validation by PCR.

Identification of Innexin family transcripts in crab and lobster nervous systems. Total RNA isolated from the crab STG and RT-PCR with poly(T) primers was used to prepare cDNA. We performed PCR on this cDNA with degenerate primers designed with published innexin sequences from *D. melanogaster*, *A. egyptii*, *H. medicinalis*, and *H. gammarus*. Three different PCR products were obtained and were further elongated with repeated 3' and 5' RACE. Full-length sequences were constructed by aligning overlapping sequences in the original PCR fragments and RACE products. These three full-length sequences were named Innexin 1 (NCBI GenBank accession no. JQ994479.1), Innexin 2 (NCBI GenBank accession no. JQ994480.1), and Innexin 3 (NCBI GenBank accession no. JQ994481.1) because they showed significant sequence similarity to mRNA sequences of innexins from multiple organisms (E values $< e^{-10}$) in a BLASTN search. Innexin 4 (NCBI GenBank accession no. KJ642222), Innexin 5 (NCBI GenBank accession no. KJ817410), and Innexin 6 (NCBI GenBank accession no. KJ817411) sequences were subsequently identified from a transcriptome sequence analysis of mixed *C. borealis* nervous system tissue. We also identified six innexin genes from the American lobster *H. americanus*, and these were named Innexin 1, Innexin 2, Innexin 3, Innexin 4, Innexin 6, and Innexin 7 based on their sequence homology to the crab innexins. The six crab and lobster innexins show considerable sequence similarity to each other (Fig. 2A). Kyte-Doolittle hydropathy profiles for protein sequences of the 12 innexins show 4 hydrophobic regions in each protein that correspond to the highly conserved transmembrane (TM) domains (Fig. 2A) found in innexins from multiple organisms (Yen and Saier 2007). All of the newly identified innexin sequences have the signature innexin motif YYQWV in the second TM domain. Additionally, these innexins have a series of amino acid residues in a highly conserved sequence considered a hallmark of innexins. These conserved sequences are as follows (with numbers in parentheses indicating number of residues between strictly conserved positions): in the region spanning TM1 and TM2 domains and the first extracellular loop S/T(17)G(4)C(13–19)C(25–92)Y(1)W(14)P(3)W and F(4)C(16–24)C(4)N(4)K(1)Y/F(3)Y/F/W in the region between the second extracellular loop and the fourth TM domain (Phelan and Starich 2001). BLAST search through the *C. borealis* transcriptome sequence also identified two other sequences that showed considerable sequence homology to the *C. borealis* Innexin 2. However, these two sequences do not contain the innexin signature motifs and are not included in the data set.

We conducted phylogenetic analysis of the newly identified *C. borealis* and *H. americanus* innexins by constructing an unrooted phylogenetic tree after sequence alignment in the CLUSTALW program against protein sequences from previously identified innexin and pannexin family proteins (Fig. 2B). The translated amino acid sequence of *C. borealis* Innexin 1 and *H. americanus* Innexin 1 are phylogenetically closest to *S. gregaria* Innexin 1 and *Drosophila* ogre proteins. Innexin 2 and Innexin 3 from both species show highest homology to *H. gammarus* Innexin 2 and Innexin 1 proteins, respectively. The Innexin 4 sequences have greatest similarity with *Drosophila* and *Anopheles* Shaking-B. Innexin 5 and Innexin 6 sequences are phylogenetically close to *Drosophila prp33*, *Schistocerca* Innexin 2, and *Bombyx* Innexin 2, while *H. americanus* Innexin 7 is most similar to *Bombyx* Innexin 3. All the vertebrate pannexins are on a different branch. Among the invertebrates, all innexins and pannexins in the Lophotrochozoan phyla (mollusca and annelida) are on one branch. Among the ecdysozoans (nematodes and arthropods), there is an apparent split between the nematode (*C. elegans*) and arthropod branches. As expected, our newly identified innexins from *C. borealis* and *H. americanus* are on the arthropod branch. Interestingly, *C. borealis* and *H. americanus* Inx1 are more related to *Drosophila* ogre and *Schistocerca* Innexin 1 than to other innexins within the species. Similarly, Inx2, Inx3, Inx4, and Inx6 in one species are more closely related to other insect innexins than to each other. This suggests that the innexin family genes differentiated from each other before the evolutionary separation between crustaceans and insects. We did not find a homolog for crab Inx5 or lobster Inx7 in other species. A phylogenetic analysis of the newly discovered innexins with all known crustacean innexin sequences (Fig. 2C) shows that, as expected, *H. americanus* Inx2 and Inx3 are more similar to *H. gammarus* Inx2 and Inx1, respectively, than they are to their crab homologs.

Within the crustaceans, the Innexins seem to be clustered into two general subfamilies (Fig. 2C), one consisting of *C. borealis* and *H. americanus* Inx1, 3, and 4 and the other consisting of *C. borealis* Inx2, 5, and 6 (*H. americanus* Inx2 and 6). We did not identify a crab ortholog to *H. americanus* Inx7, and it has sequence features distinct from any of the other crustacean innexins. However, the apparent clustering of this Inx7 with *Penaeus monodon* (the Asian tiger shrimp) Inx1, despite the fact that *Penaeus* and *Homarus/Cancer* belong to distinct monophyletic suborders (De Grave et al. 2009), suggests that either the *C. borealis* transcriptome identification of Innexins was incomplete or this ortholog was lost in *C. borealis*. Similar assessments can be made for the lack of an ortholog to *C. borealis* Inx5 in *H. americanus*.

Tissue- and cell type-specific expression of innexin genes in the crab. Our tissue RT-PCR screen revealed heterogeneity in the expression of all six innexin genes in the crab *C. borealis* across both muscle and nervous system samples (Fig. 3A). Skeletal muscle expressed all six innexins with apparent equal intensity, while heart muscle expressed almost exclusively Inx5. The brain and CoG samples expressed all six innexins with fairly high intensity. The OG expressed Inx1, Inx2, Inx3, and Inx5 most prominently, with Inx6 expression also detected while Inx4 was only faintly detectable. Finally, the STG as a whole strongly expressed Inx1, Inx2, Inx3, and Inx5 but showed much weaker Inx4 and Inx6 expression.

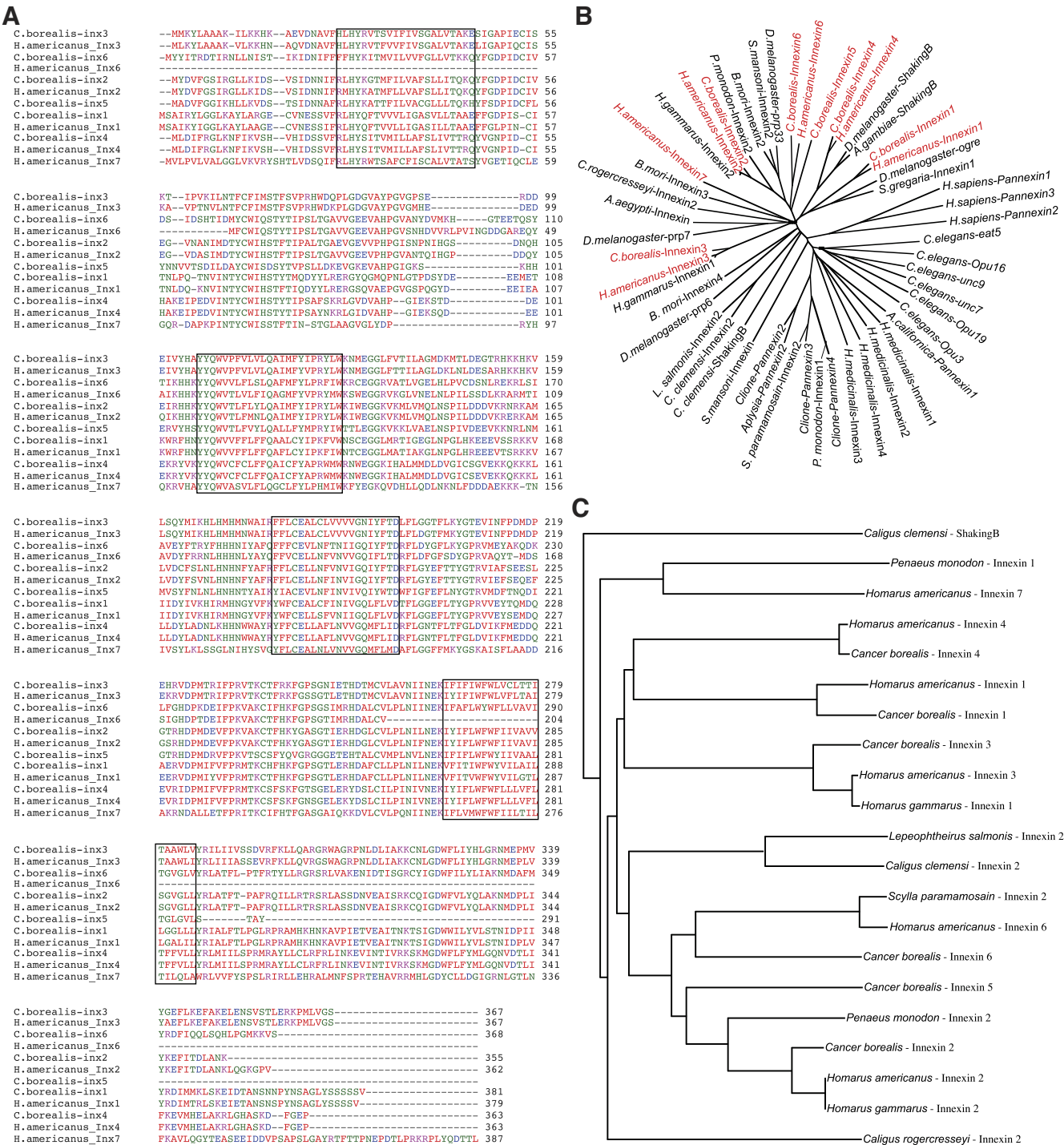


Fig. 2. Identification and analysis of innixin protein sequences. A: sequence alignment of *Cancer borealis* and *Homarus americanus* Innixin proteins based on mRNA isolated from the STG. Black boxes represent transmembrane domains. B: unrooted phylogenetic tree showing the relationship between *C. borealis* and *H. americanus* innixins with other innixins and pannexins. C: rooted tree describing the relationship among known crustacean innixins with the newly described *H. americanus* and *C. borealis* sequences.

To better determine the expression patterns of innexins in the STG, we performed single-cell RT-PCR for each of the innixin subtypes from identified neurons of the pyloric network [pyloric dilator (PD), LP, pyloric constrictor (PY), ventral dilator (VD), IC, and lateral posterior gastric (LPG)]. A representative gel for transcript detection is shown in Fig. 3B. The data show variability of innixin expression within cells of the same type but also demonstrate cell type-specific expres-

sion of different innexin genes. *Inx1–3* are ubiquitously expressed in all cells of the pyloric network. We detected *Inx1*, *Inx2*, and *Inx3* in all replicates of all six cell types, with one exception (4 of 5 VD neurons were *Inx1* positive). Not only were these three the most commonly detected, but the band intensities were always strong (see Fig. 3B), suggesting substantive expression. *Inx4* showed clear heterogeneity across cell types: LP, PY, PD, and IC all expressed *Inx4*, while in five

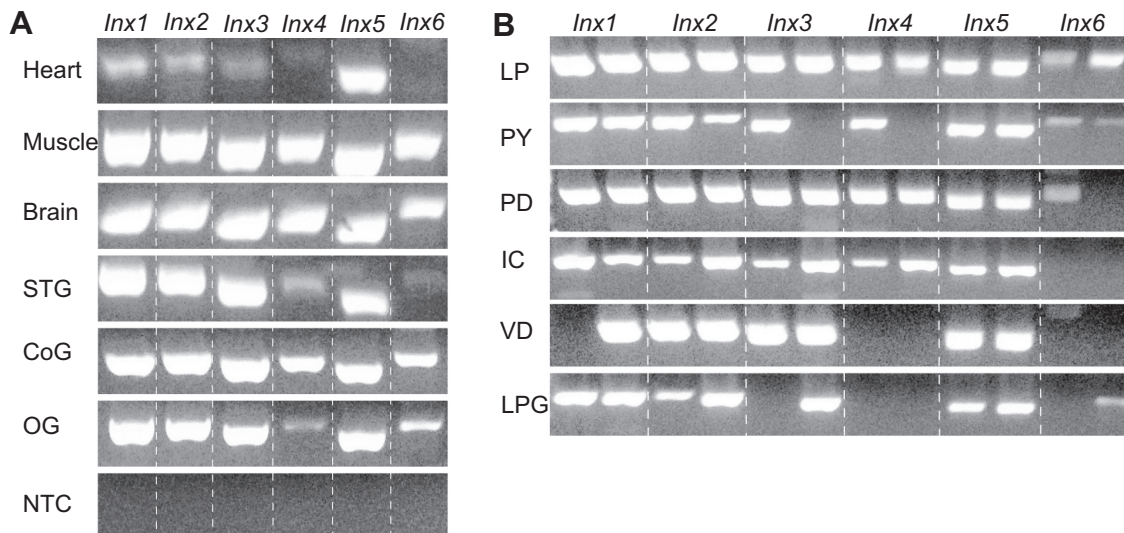


Fig. 3. Tissue- and cell type-specific expression of innexin in the crab. *A*: RT-PCR gels showing expression of Innexins 1–6 in different tissues in the crab. OG, esophageal ganglia; NTC, no template control. *B*: expression of Innexins 1–6 in 6 different cell types in the STG.

of five VD and LPG cells tested we failed to detect *Inx6* transcript. *Inx5* was detected in all lateral pyloric (LP) cells but expressed in four of five PD and IC cells, three of five PY, VD, and gastric mill (GM) cells, and two of five LPG cells. Finally, *Inx6* expression was detected in three of five LP, PY, LPG, and GM cells, two of five PD cells, and only one cell each for IC and VD. Taken together, these data demonstrate that there is a cell-specific pattern of innexin expression across cell types in the pyloric network. It is not known whether those cell types for which only a subset of the five replicates tested showed expression represent biological variability across individuals for innexin expression or a technical detection threshold phenomenon.

Because *Inx1* and *Inx3* were two of the most prominently expressed innexins in the STG neurons (see Fig. 3*B*), we performed *in situ* hybridization with *Inx1* and *Inx3* LNA probes on the STG. Experiments with antisense probes show that both *Inx1* (Fig. 4, *A–C*) and *Inx3* (Fig. 4, *D–F*) transcripts are expressed in a majority of cells in the STG. This staining was often visible as a ring around the nucleus. *In situ* hybridization with a sense probe for *Inx1* or *Inx3* did not show any staining (data not shown). *Inx1* transcripts were expressed on average in 20.16 ± 2.97 cells in the STG ($n = 19$ preparations), while *Inx3* transcripts were expressed on average in 16.46 ± 3.17 cells ($n = 11$ preparations). The number of cells expressing *Inx1* transcripts is significantly higher than that of those expressing *Inx3* mRNA ($P = 0.003$, *t*-test). The expression of both *Inx1* and *Inx3* mRNA is not restricted to specific cell types in the STG. For every identified cell type, 50–100% of the cells tested expressed either *Inx1* or *Inx3* transcripts (Fig. 4, *C* and *F*).

In situ hybridization experiments do not provide quantitative information about transcript levels in each cell type. To get mRNA copy numbers from individual cells, we performed RT-qPCR with *Inx1*, *Inx2*, and *Inx3* primers on identified single cells isolated from the STG. These experiments further confirmed our *in situ* hybridization results because all cells on which RT-qPCR was performed expressed the three innexins (Table 1).

Characterization of Innexin expression in PD and LPG cells in crab STG. To characterize the expression of Innexins 1, 2, and 3 within an individual cell, we did further analysis on RT-qPCR data from PD and LPG neurons. Every STG has two PD and two LPG neurons. The two PD neurons form electrical synapses with each other and the anterior burster (AB) neuron to make up the pacemaker unit for the pyloric rhythm. Additionally, the PD neurons form electrical synapses with the two LPG neurons, while the LPG neurons form electrical synapses with each other and also with the VD neuron (Fig. 1*B*). The evidence for electrical synapses in the PD and LPG neurons make them ideal candidates for studying the expression of gap junction genes.

Comparison of innexin gene expression within individual PD neurons shows no correlation between mRNA copy numbers for *Inx1*, *Inx2*, or *Inx3* transcripts (for *Inx1* against *Inx2*, $R^2 = 0.102$, $n = 38$; for *Inx1* against *Inx3*, $R^2 = 0.019$, $n = 33$; for *Inx2* against *Inx3*, $R^2 = 0.035$, $n = 33$; $P > 0.1$ for all). However, the *Inx1* mRNA copy number was significantly higher than the mRNA copy number for *Inx2* and *Inx3* ($P = 0.0004$, $n = 30$, 1-way ANOVA with Bonferroni means comparison). No significant trend was present in mRNA copy number between *Inx2* and *Inx3*.

We observed a significant correlation between *Inx1* mRNA copy numbers in the coupled PD cells from the same STG ($R^2 = 0.79$, $P < 0.001$, $n = 12$ pairs; Fig. 5*A*). However, there was no apparent correlation in the expression of *Inx2* ($R^2 = 0.18$, $P > 0.1$, $n = 12$ pairs) or *Inx3* ($R^2 = 0.041$, $P > 0.1$, $n = 12$ pairs) genes in coupled PD cells.

Similar to PD neurons, LPG neurons showed no correlation between mRNA copy numbers for *Inx1*, *Inx2*, or *Inx3* transcripts (for *Inx1* against *Inx2*, $R^2 = 0.0001$, $n = 26$; for *Inx1* against *Inx3*, $R^2 = 0.0951$, $n = 25$; for *Inx2* against *Inx3*, $R^2 = 0.0868$, $n = 25$; $P > 0.1$ for all). Mean comparisons show that in LPG cells *Inx3* mRNA copy number was significantly lower than *Inx1* but not *Inx2* ($P = 0.00094$, $n = 24$, 1-way ANOVA with Bonferroni means comparison), while there was no significant difference between *Inx1* and *Inx2* transcript levels. Similar to PD cells, there was a significant correlation between

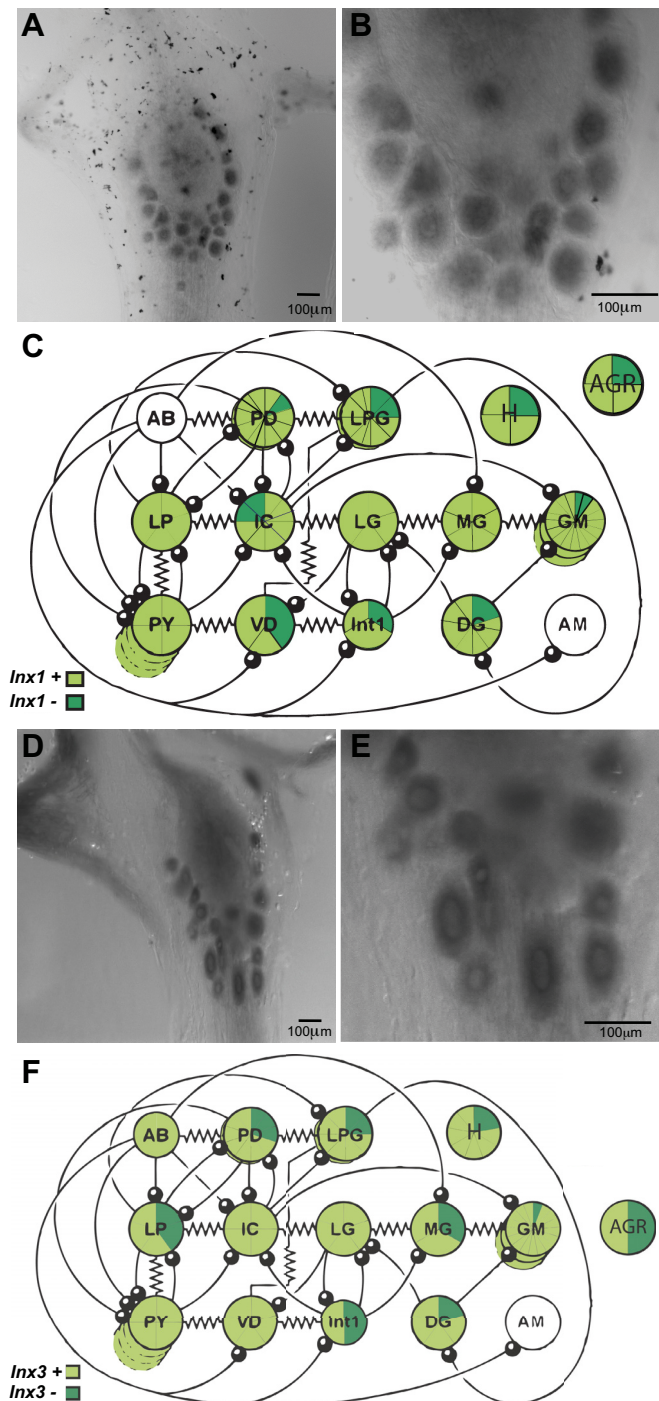


Fig. 4. *In situ* hybridization pattern for Innexin mRNA in the STG. **A** and **B**: *In situ* hybridization for *Inx1* mRNA at low (**A**) and higher (**B**) magnification. **C**: summary schematic of the STG circuit with the expression pattern of *Inx1* mRNA. Each cell is represented as a pie chart, with light green sections showing the number of cells positive for *Inx1* mRNA and dark green sections the number of *Inx1*-negative cells. **D** and **E**: *In situ* hybridization for *Inx3* mRNA at low (**D**) and higher (**E**) magnification. **F**: same as **C** but for *Inx3* mRNA. AGR, anterior gastric receptor; H, hyperpolarizing cell.

Inx1 mRNA copy number in the two LPG cells within the same STG ($R^2 = 0.81$, $P = 0.003$, $n = 7$ pairs; Fig. 5B) while no correlation was observed for the expression of *Inx2* ($R^2 = 0.47$, $P = 0.06$, $n = 7$ pairs) or *Inx3* ($R^2 = 0.037$, $P > 0.1$, $n = 7$ pairs) mRNA. When the expression levels of the three innexins

are compared between PD and LPG cells, we find no distinct pattern of gene expression separating the two cell types (Fig. 5C).

Rectifying and nonrectifying electrical synapses are present in STG. It is well established that some electrical synapses are not simple bidirectional channels allowing for the free flow of molecules in both directions. Many different networks have rectifying electrical synapses that facilitate conductance in one direction, and recent experiments from *Drosophila* and goldfish suggest correlations between rectifying electrical synapses and the molecular identity of the gap junction protein being expressed (Phelan et al. 2008; Rash et al. 2013). We further looked into this question by measuring coupling coefficients (CCs) in PD-LPG and PD-PD pairs of electrically coupled cells. This was done by injecting a series of depolarizing and hyperpolarizing current steps in one cell and simultaneously recording the change in membrane potential in the injected cell and the cells coupled to it. The coupling coefficient was calculated as the ratio of the change in voltage in the second cell to the voltage change in the injected cell (METHODS).

We looked at the coupling strength and directionality of the electrical synapse between the PD and LPG cells (Fig. 6). The PD-LPG pair of cells showed a distinct directionality, and for every PD-LPG pair tested the apparent coupling coefficient was larger when hyperpolarizing currents were injected in the LPG cell compared with hyperpolarizing current injections in the coupled PD cell ($CC_{PD-LPG} = 0.097 \pm 0.078$; $CC_{LPG-PD} = 0.248 \pm 0.14$, $n = 33$ pairs; $P = 0.000015$ by paired *t*-test; Fig. 6C). This suggests that electrical synapses between PD and LPG cells are rectifying and a hyperpolarizing current is preferentially transmitted from the LPG cell to the PD cell. The strength of the apparent coupling coefficient is dependent on the properties of the electrical synapse as well as the input resistance of the two cells (Veruki and Hartveit 2002). For these pairs of PD and LPG cells, we did not find any significant difference in the input resistance values (input resistance: PD = 6.36 ± 3.22 M Ω , LPG = 5.21 ± 3.02 M Ω ; $n = 33$ pairs; $P = 0.106$ by paired *t*-test). Additionally, we found that a depolarizing current was preferentially transmitted from the PD cell to the LPG cell ($CC_{PD-LPG} = 0.163 \pm 0.081$; $CC_{LPG-PD} = 0.093 \pm 0.068$, $n = 30$ pairs; $P = 0.0024$ by paired *t*-test; Fig. 6, **A** and **B**). For example, in the traces shown in Fig. 6A, when the PD cell was depolarized this change in voltage caused a greater depolarizing change in the membrane potential of a coupled LPG cell than when the same cell was hyperpolarized. Conversely, traces in Fig. 6B show that when the LPG cell was depolarized, the corresponding voltage change in the PD cell was smaller than when the LPG cell was hyperpolarized (traces in Fig. 6, **A** and **B**, are from the same pair of cells). While these results strongly suggest that the PD-LPG synapse is rectifying, the fact that both PD and LPG cells are electrically connected to multiple other cells makes it impossible to measure the exact coupling coefficient values in both directions, or to directly measure junctional conductance.

The two PD cells in the STG are also coupled to each other (Fig. 7; CC = 0.17 ± 0.079 ; $n = 32$ pairs). PD cells within an STG preparation were named PD1 and PD2 based on the order in which they were identified during the experiment. For every PD-PD pair tested, there was no significant difference in

Table 1. Innexin 1, 2, and 3 mRNA copy number per cell obtained from single-cell RT-qPCR in STG cells

Cell Type	Innixin 1	Innixin 2	Innixin 3
PD	5,199 ± 4,268 (n = 36)	2,443 ± 4,479 (n = 35)	1,104 ± 1,542 (n = 31)
LPG	6,259 ± 6,948 (n = 26)	3,099 ± 3,620 (n = 25)	743 ± 607 (n = 25)
GM	4,203 ± 3,519 (n = 6)	1,122 ± 588 (n = 6)	231 ± 271 (n = 3)
PY	4,796 ± 1,860 (n = 7)	1,535 ± 654 (n = 7)	1,963 ± 3,300 (n = 5)
LP	2,926 ± 1,564 (n = 8)	1,481 ± 1,307 (n = 8)	1,743 ± 1,669 (n = 7)
VD	3,687 ± 2,868 (n = 8)	812 ± 590 (n = 8)	1,337 ± 2,341 (n = 7)

Values are means ± SD. STG, stomatogastric ganglion; PD, pyloric dilator; LPG, lateral posterior gastric; GM, gastric mill; PY, pyloric constrictor; LP, lateral pyloric; VD, ventral dilator.

coupling coefficient when a hyperpolarizing current was injected in PD1 or in PD2 in the same STG preparation (Fig. 7B; $CC_{PD1-PD2} = 0.19 \pm 0.08$, $CC_{PD2-PD1} = 0.18 \pm 0.073$; n = 15 preparations; P = 0.84 by paired t-test).

So far, we have shown pairwise coupling between PD-PD and PD-LPG cells. However, the STG circuit is more like a syncytium where any given cell is electrically coupled to multiple cells of different cell types. Is there any correlation between the coupling coefficients of different electrical synapses formed by the same cell? To address this, we did simultaneous recordings from the two PD cells and one or both LPG cells in a preparation. Because the two PD and two LPG cells are all electrically coupled with each other, this allowed us to measure multiple coupling coefficients at the same time. For example, a series of current injections in the PD1 cell allows us to simultaneously record $CC_{PD1-PD2}$, $CC_{PD1-LPG1}$, and $CC_{PD1-LPG2}$ (Fig. 8, A–D). These experiments show that there is no correlation between CC_{PD-PD} and CC_{PD-LPG} for any given PD cell, suggesting that the strength of electrical coupling is not entirely dependent on membrane properties and individual synapses from a given neuron might be independently regulated (Fig. 8E; for $CC_{PD1-PD2}$ against $CC_{PD1-LPG}$, $R^2 = 0.0123$, n = 14; for $CC_{PD1-PD2}$ against $CC_{LPG-PD1}$, $R^2 = 0.081$, n = 13; for $CC_{PD2-PD1}$ against $CC_{PD2-LPG}$, $R^2 = 0.0337$, n = 14; for $CC_{PD2-PD1}$ against $CC_{LPG-PD2}$, $R^2 = 0.1025$, n = 14).

Similar to the PD-LPG synapse, the PY-LP synapse appears to be rectifying ($CC_{LP-PY} = 0.106 \pm 0.056$, n = 4; $CC_{PY-LP} = 0.17 \pm 0.13$, n = 3). The AB-PD synapse also seems to be directional, with the AB-PD synapse being stronger than the PD-AB synapse when a hyperpolarizing current is injected ($CC_{AB-PD} = 0.32 \pm 0.06$; $CC_{PD-AB} = 0.202 \pm 0.021$; n = 2 pairs).

Innixin expression is not correlated with apparent strength of electrical coupling in PD-LPG synapse. Previous studies have shown that the molecular identity of the gap junction proteins in two cells might affect the strength and directionality of electrical coupling between those cells (Phelan et al. 2008; Rash et al. 2013). The presence of distinct, easily identifiable cells and the ease of performing single-cell molecular biology on these cells make the STG a good preparation for correlating the electrophysiological and molecular biological properties of a particular cell. Because the PD-LPG electrical synapse appeared to be rectifying and rectifying synapses are often associated with the presence of asymmetric or heterotypic gap junctions, we further investigated whether there was any correlation between the coupling coefficient and directionality of these electrical synapses and the expression levels of innixin mRNAs. Most of the coupling coefficient and RT-qPCR data presented above were obtained from the same identified PD and LPG cells, allowing us to investigate any possible correlations within cells.

We looked at the correlation between mRNA copy numbers of *Inx1*, *Inx2*, and *Inx3* genes with the coupling coefficient between PD and LPG cells. We did not find any correlation between CC_{PD-LPG} and the expression of the three innixin genes in the presynaptic PD cell (for *Inx1*, $R^2 = 0.037$; for *Inx2*, $R^2 = 0.26$; for *Inx3*, $R^2 = 0.024$; for all n = 14 and P > 0.1) or the postsynaptic LPG cell (for *Inx1*, $R^2 = 0.0015$; for *Inx2*, $R^2 = 0.01$; for *Inx3*, $R^2 = 0.05$; for all n = 15 and P > 0.1). Similarly, when we investigated the correlation for coupling coefficient in the opposite direction, we did not find any correlation between CC_{LPG-PD} and innixin expression in the PD (for *Inx1*, $R^2 = 0.075$; for *Inx2*, $R^2 = 0.0025$; for *Inx3*, $R^2 = 0.0015$; for all n = 13 and P > 0.1) or LPG (for *Inx1*,

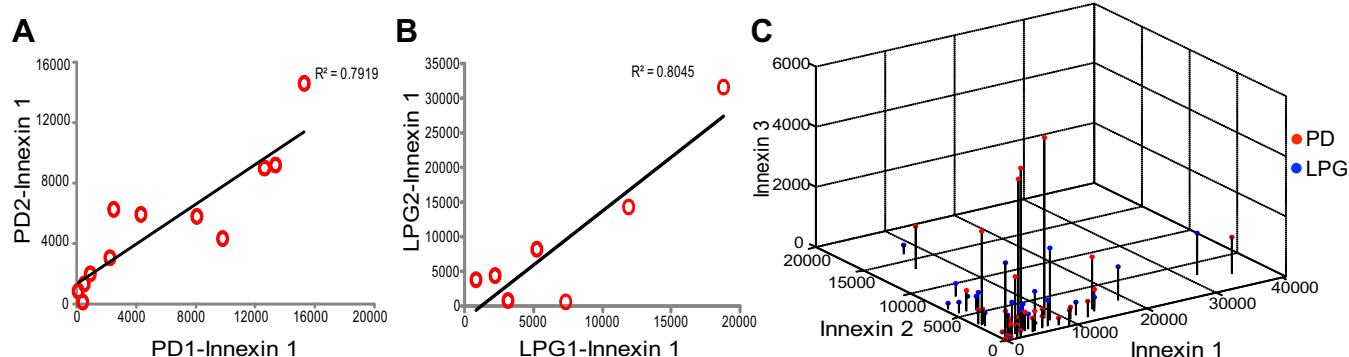


Fig. 5. Expression of innexins in PD and LPG cells. A: correlation between *Inx1* mRNA expressed in the 2 PD cells expressed within the same STG. B: correlation between *Inx1* mRNA expressed in the 2 LPG cells in the same STG. C: distribution in 3D space of mRNA levels for 3 innexins in PD and LPG cells.

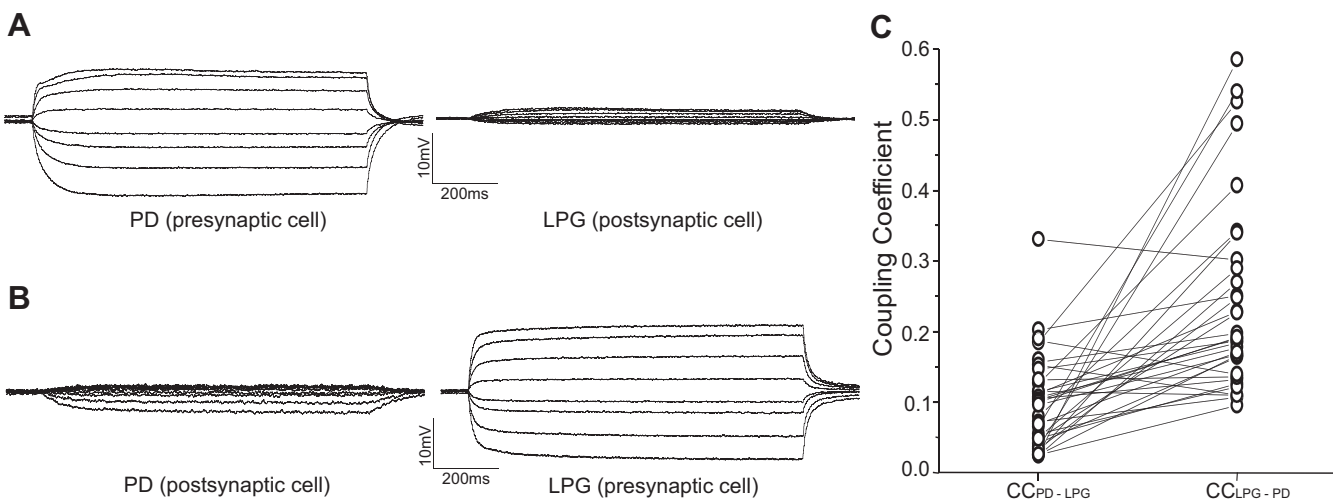


Fig. 6. The PD-LPG electrical synapse is asymmetric. *A*: example traces from electrically coupled PD and LPG cells after a series of current steps are injected in the PD cell. *B*: same as *A* but with a series of current steps injected in the LPG cell. *C*: scatterplot of coupling coefficients (CC_{PD-LPG} and CC_{LPG-PD}) in all recorded pairs.

$R^2 = 0.06$; for *Inx2*, $R^2 = 0.21$; for *Inx3*, $R^2 = 0.029$; for all $n = 14$ and $P > 0.1$ cells.

DISCUSSION

Electrical synapses are ubiquitous in both vertebrate and invertebrate nervous systems. A number of elegant studies over the last sixty years have extensively studied the biophysical properties of these synapses. As the innixin and connexin proteins forming these gap junctions have been identified, it has become evident that the biophysical properties of electrical synapses can be dependent on the gap junction proteins forming that synapse (Phelan et al. 2008; Rash et al. 2013). In this study, we used the intact stomatogastric nervous system of the crab to simultaneously study coupling coefficient and innixin gene expression at the single-cell level.

We initially isolated three innixin genes in the crab STG by RT-PCR and identified three more innixins by analysis of the transcriptome sequence. This number is lower than the number of innixins found in other invertebrates (Curtin et al. 1999; Kandarian et al. 2012; Starich et al. 2001; Stebbings et al. 2002). Our extensive search of the transcriptome sequence provided two other innixin-like sequences that are missing the hallmark motifs of an innixin. In light of these results, we are fairly confident that only six innixins are expressed in neuronal tissue. However, both our RT-PCR and transcriptome studies were restricted to neural tissue in adult crabs. It is possible that there are more innixin genes expressed in other tissues of the crab or at different developmental stages. Additionally, our

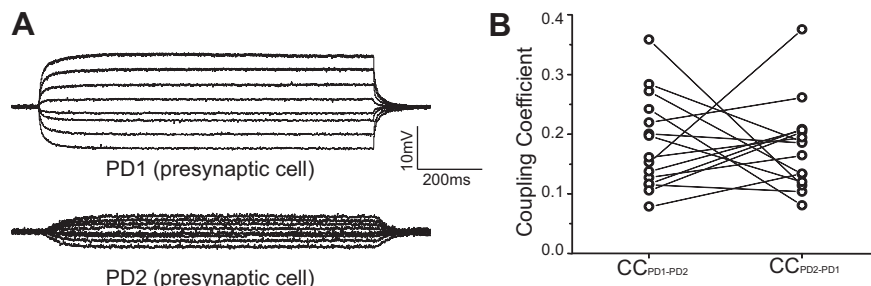
conclusions do not preclude the presence of splice variants to provide further variability to innixin gene expression.

In situ hybridization and RT-PCR experiments on identified STG cells showed that most of the cells in the STG express all six innixins. We did not find any correlation between the mRNA copy numbers of Innexins 1, 2, and 3 within individual cells, suggesting that they may be independently regulated, at least at the level of transcription. We identified six innixin genes in the crab STG, but the qPCR results are only from three innixins—*Inx1*, *Inx2*, and *Inx3*. Thus a lack of correlation in our experiments can only be used to draw conclusions about these particular innixins. It is possible that other gap junction proteins in the STG are coregulated. Interestingly, *Inx1* expression was significantly correlated in the two electrically coupled PD cells and two LPG cells from the same STG. This is similar to previous results that show a correlation between the expression of two ion channels, I_A (shal) and I_H (HCN), in coupled PD neurons (Schulz et al. 2006). There is ample evidence for activity-dependent gene expression in neurons (Barth et al. 2004; Golowasch et al. 1999; Temporal et al. 2014), and because electrically coupled pairs of PD or LPG cells have very similar activity, it is possible that they have similar gene expression patterns. Additionally, small molecules like cyclic nucleotides, calcium ions, and inositol 1,4,5-trisphosphate can pass through gap junctions (Bevans et al. 1998; Saez et al. 1989). It is possible that such shared molecules regulate gene expression in coupled cells.

We were able to electrophysiologically measure the apparent coupling coefficient and then isolate these cells to perform

Downloaded from on February 4, 2015

Fig. 7. The PD-PD electrical synapse is nonrectifying. *A*: example traces from electrically coupled PD cells in the same STG after a series of current steps are injected in PD1 cell. *B*: scatterplot of $CC_{PD1-PD2}$ and $CC_{PD2-PD1}$ in all recorded pairs.



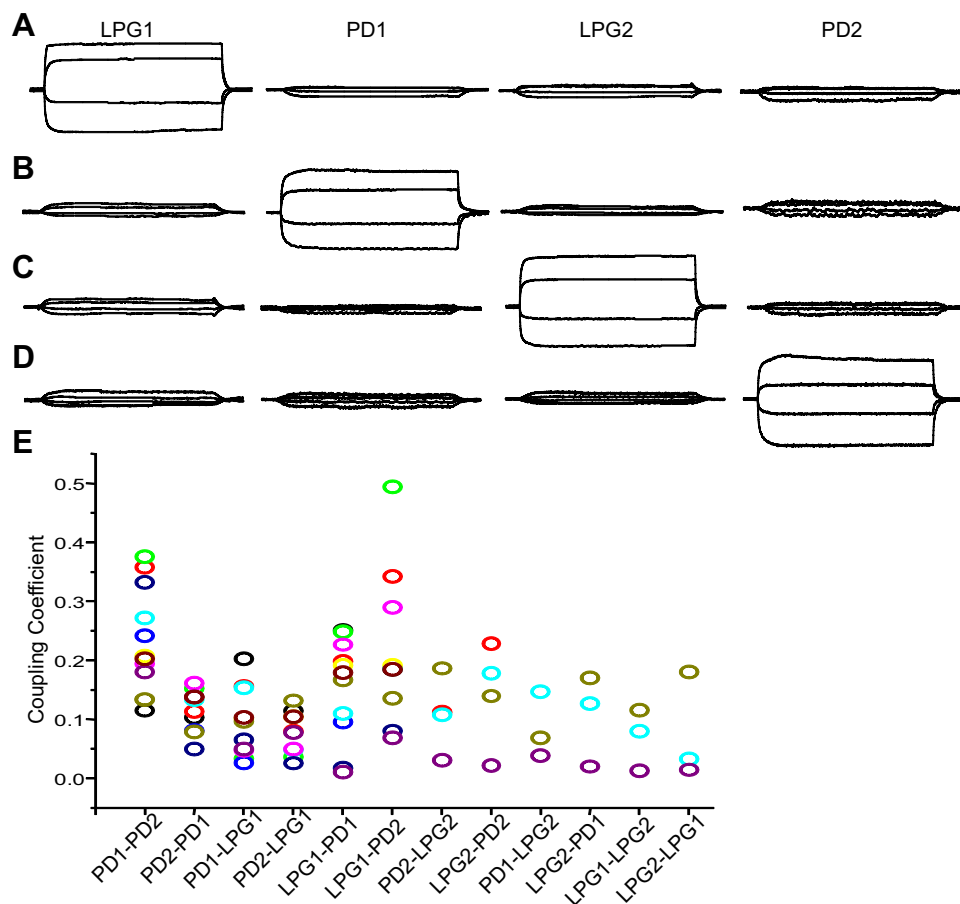


Fig. 8. A–D: example traces showing electrical coupling recorded simultaneously from both PD and LPG cells in the same STG when current was injected in LPG1 (A), PD1 (B), LPG2 (C), and PD2 (D) cells. E: coupling coefficient for all combinations of PD and LPG cells within an STG. All data points in a given color were recorded from the same STG.

RT-qPCR for levels of innixin genes. However, we did not see any correlation between electrical coupling and the levels of innixin genes in coupled cells. There can be many reasons for the lack of these correlations. There are multiple steps, such as splicing, translation, posttranslational modifications, and protein trafficking, between mRNA production and physiological output. Given the large number of points at which a gene or protein can be regulated, our results may not be surprising. Additionally, many cells in the STG circuit are highly connected to each other by gap junctions. Because the electrophysiological experiments were conducted in an intact circuit and the recorded cells were not electrically isolated from other coupled cells in the circuit, it is possible that while the expression of a particular innixin might not be correlated with the strength of coupling in the tested pair, it might very well be correlated to the strength of all electrical synapses formed by that cell with different cells in the circuit.

This study shows that PD-PD and PD-LPG synapses show significant electrical coupling. We did not try to measure the junctional conductance between two cells. A number of elegant studies have directly measured junctional conductance in voltage clamp (Harris et al. 1981; Lasater and Dowling 1985; Phelan et al. 1998; Spray et al. 1986) or indirectly calculated the value in current clamp (Devor and Yarom 2002; Landisman and Connors 2005; Rash et al. 2013). However, these studies were restricted to electrical synapses between two isolated, identical cells that only form electrical synapses with each other. As is evident from Fig. 1*B*, neurons in the STG are connected to multiple cells of different types through electrical

synapses. Thus electrical coupling in the STG forms an extended distributed circuit, and it is not possible to simplify the coupling within the STG to an isolated two-neuron system as required by the above-mentioned methods. Even methods that take into account a single neuron electrically coupled to multiple neurons within a network assume that all those other neurons are coupled only to that central neuron and not to each other and that all electrically coupled neurons are homogeneous with identical electrical properties (Amitai et al. 2002). Previous STG literature and our data (Fig. 8) show that this is not true for electrical coupling within the STG—these neurons have multiple combinations of electrical synapses between cells of different sizes and membrane properties. Even though the junctional conductance is a more rigorous biophysical measurement of electrical coupling strength, it is impossible to obtain in an intact nervous system like the stomatogastric nervous system, and we restricted ourselves to the more directly measurable coupling coefficient.

The coupling coefficients between the PD and LPG electrical synapse show an asymmetry in the strength of these synapses such that a depolarizing current flows preferentially from the PD to LPG cell while a hyperpolarizing current flows preferentially in the opposite direction. This can have implications for the function of the STG. For example, the STG circuit generates two distinct rhythms—the constantly active, fast pyloric rhythm and the episodically active, slow gastric rhythm. In the absence of the gastric rhythm, LPG neurons fire closely in time with the PD neurons, to the extent that they were originally believed to be PD neurons (Hooper et al. 1986).

However, LPG neurons innervate gastric mill muscles, and in the presence of rhythmic gastric activity they can fire in time with the gastric rhythm (Weimann et al. 1991). Our results suggest that the coupling between PD and LPG neurons should be weaker when the LPG neuron is depolarized. It is tempting to speculate that depolarization of LPG neurons by the activation of the gastric rhythm can help in decoupling LPG cells from the pyloric rhythm. Modeling studies have shown that regulation of rectifying gap junctions can help neurons to switch between two different circuits (Gutierrez et al. 2013; Gutierrez and Marder 2013), and it is possible that the regulation of the PD-LPG synapses serves similar functions. Additionally, the strength and directionality of electrical synapses can be regulated by neuromodulators and changes in membrane properties (Curti and Pereda 2004; Kothmann et al. 2009; O'Brien 2014). The LPG-PD synapse may serve as a site for such regulation and help the network respond to changing sensory inputs.

Although the presence of electrical synapses in the crustacean STG has been known for many years, we are just beginning to understand the molecular underpinnings of these synapses. Our results show that multiple innexins are simultaneously expressed in a given STG neuron. This leads to some intriguing questions. Do cells partition different innexins to different postsynaptic partners? Do STG neurons form heteromeric gap junctions containing more than one innixin? Are different innexins present in different subcellular locations? Innixin-specific antibodies based on sequences identified in this study will help in answering such questions and will provide interesting insights into circuit function within the STG.

ACKNOWLEDGMENTS

We thank Dr. Dirk Bucher and Veronica Garcia for providing the in situ hybridization protocol.

GRANTS

This research was supported by National Institutes of Health Grants NS-17813 and MH-46742.

DISCLOSURES

No conflicts of interest, financial or otherwise, are declared by the author(s).

AUTHOR CONTRIBUTIONS

Author contributions: S.S., D.J.S., and E.M. conception and design of research; S.S. and K.M.L. performed experiments; S.S., D.J.S., and K.M.L. analyzed data; S.S., D.J.S., K.M.L., and E.M. interpreted results of experiments; S.S., D.J.S., and K.M.L. prepared figures; S.S. drafted manuscript; S.S., D.J.S., and E.M. edited and revised manuscript; S.S., D.J.S., K.M.L., and E.M. approved final version of manuscript.

REFERENCES

- Amitai Y, Gibson JR, Beierlein M, Patrick SL, Connors BW, Golomb D. The spatial dimensions of electrically coupled networks of interneurons in the neocortex. *J Neurosci* 22: 4142–4152, 2002.
- Anava S, Rand D, Zilberstein Y, Ayali A. Innixin genes and gap junction proteins in the locust frontal ganglion. *Insect Biochem Mol Biol* 39: 224–233, 2009.
- Auerbach AA, Bennett MV. A rectifying electrotonic synapse in the central nervous system of a vertebrate. *J Gen Physiol* 53: 211–237, 1969.
- Bao L, Locovei S, Dahl G. Pannexin membrane channels are mechanosensitive conduits for ATP. *FEBS Lett* 572: 65–68, 2004.
- Baro DJ, Cole CL, Harris-Warrick RM. RT-PCR analysis of shaker, shab, shaw, and shal gene expression in single neurons and glial cells. *Receptors Channels* 4: 149–159, 1996.
- Baro DJ, Cole CL, Zarrin AR, Hughes S, Harris-Warrick RM. Shab gene expression in identified neurons of the pyloric network in the lobster stomatogastric ganglion. *Receptors Channels* 2: 193–205, 1994.
- Barth AL, Gerkin RC, Dean KL. Alteration of neuronal firing properties after *in vivo* experience in a FosGFP transgenic mouse. *J Neurosci* 24: 6466–6475, 2004.
- Bauer R, Loer B, Ostrowski K, Martini J, Weimbs A, Lechner H, Hoch M. Intercellular communication: the *Drosophila* innixin multiprotein family of gap junction proteins. *Chem Biol* 12: 515–526, 2005.
- Beierlein M, Gibson JR, Connors BW. A network of electrically coupled interneurons drives synchronized inhibition in neocortex. *Nat Neurosci* 3: 904–910, 2000.
- Bem T, Le Feuvre Y, Rinzel J, Meyrand P. Electrical coupling induces bistability of rhythms in networks of inhibitory spiking neurons. *Eur J Neurosci* 22: 2661–2668, 2005.
- Bevans CG, Kordel M, Rhee SK, Harris AL. Isoform composition of connxin channels determines selectivity among second messengers and uncharged molecules. *J Biol Chem* 273: 2808–2816, 1998.
- Beyer EC, Paul DL, Goodenough DA. Connexin43: a protein from rat heart homologous to a gap junction protein from liver. *J Cell Biol* 105: 2621–2629, 1987.
- Bittman K, Becker DL, Cicirata F, Parnavelas JG. Connexin expression in homotypic and heterotypic cell coupling in the developing cerebral cortex. *J Comp Neurol* 443: 201–212, 2002.
- Blagburn JM, Alexopoulos H, Davies JA, Bacon JP. Null mutation in shaking-B eliminates electrical, but not chemical, synapses in the *Drosophila* giant fiber system: a structural study. *J Comp Neurol* 404: 449–458, 1999.
- Blitz DM, Christie AE, Coleman MJ, Norris BJ, Marder E, Nusbaum MP. Different proctolin neurons elicit distinct motor patterns from a multifunctional neuronal network. *J Neurosci* 19: 5449–5463, 1999.
- Bukauskas FF, Angele AB, Verselis VK, Bennett MV. Coupling asymmetry of heterotypic connexin 45/connexin 43-EGFP gap junctions: properties of fast and slow gating mechanisms. *Proc Natl Acad Sci USA* 99: 7113–7118, 2002.
- Caspar DL, Goodenough DA, Makowski L, Phillips WC. Gap junction structures. I. Correlated electron microscopy and x-ray diffraction. *J Cell Biol* 74: 605–628, 1977.
- Connors BW, Long MA. Electrical synapses in the mammalian brain. *Annu Rev Neurosci* 27: 393–418, 2004.
- Cruciani V, Mikalsen SO. Evolutionary selection pressure and family relationships among connexin genes. *Biol Chem* 388: 253–264, 2007.
- Curti S, Pereda AE. Voltage-dependent enhancement of electrical coupling by a subthreshold sodium current. *J Neurosci* 24: 3999–4010, 2004.
- Curtin KD, Zhang Z, Wyman RJ. *Drosophila* has several genes for gap junction proteins. *Gene* 232: 191–201, 1999.
- Deans MR, Gibson JR, Sellitto C, Connors BW, Paul DL. Synchronous activity of inhibitory networks in neocortex requires electrical synapses containing connexin36. *Neuron* 31: 477–485, 2001.
- De Grave S, Pentcheff ND, Ahyong ST, Chan TY, Crandall KA, Dworschak PC, Felder DL, Feldmann RM, Fransen CH, Goulding LY, Lemaitre R, Low ME, Martin JW, Ng PK, Schweitzer CE, Tan SH, Tshudy D, Wetzer R. A classification of living and fossil genera of decapod crustaceans. *Raffles Bull Zool* 21: 1–109, 2009.
- Devor A, Yarom Y. Electrotonic coupling in the inferior olivary nucleus revealed by simultaneous double patch recordings. *J Neurophysiol* 87: 3048–3058, 2002.
- Dickinson PS, Marder E. Peptidergic modulation of a multioscillator system in the lobster. I. Activation of the cardiac sac motor pattern by the neuropeptides proctolin and red pigment-concentrating hormone. *J Neurophysiol* 61: 833–844, 1989.
- Ducret E, Alexopoulos H, Le Feuvre Y, Davies JA, Meyrand P, Bacon JP, Fenelon VS. Innexins in the lobster stomatogastric nervous system: cloning, phylogenetic analysis, developmental changes and expression within adult identified dye and electrically coupled neurons. *Eur J Neurosci* 24: 3119–3133, 2006.
- Ducret E, Le Feuvre Y, Meyrand P, Fenelon VS. Removal of GABA within adult modulatory systems alters electrical coupling and allows expression of an embryonic-like network. *J Neurosci* 27: 3626–3638, 2007.

- Dykes IM, Macagno ER.** Molecular characterization and embryonic expression of innexins in the leech *Hirudo medicinalis*. *Dev Genes Evol* 216: 185–197, 2006.
- Edwards DH, Heitler WJ, Leise EM, Fricke RA.** Postsynaptic modulation of rectifying electrical synaptic inputs to the LG escape command neuron in crayfish. *J Neurosci* 11: 2117–2129, 1991.
- Furshpan EJ, Potter DD.** Transmission at the giant motor synapses of the crayfish. *J Physiol* 145: 289–325, 1959.
- Golowasch J, Abbott LF, Marder E.** Activity-dependent regulation of potassium currents in an identified neuron of the stomatogastric ganglion of the crab *Cancer borealis*. *J Neurosci* 19: RC33, 1999.
- Gutierrez GJ, Marder E.** Rectifying electrical synapses can affect the influence of synaptic modulation on output pattern robustness. *J Neurosci* 33: 13238–13248, 2013.
- Gutierrez GJ, O'Leary T, Marder E.** Multiple mechanisms switch an electrically coupled, synaptically inhibited neuron between competing rhythmic oscillators. *Neuron* 77: 845–858, 2013.
- Harris AL, Spray DC, Bennett MV.** Kinetic properties of a voltage-dependent junctional conductance. *J Gen Physiol* 77: 95–117, 1981.
- Hooper SL, Marder E.** Modulation of the lobster pyloric rhythm by the peptide proctolin. *J Neurosci* 7: 2097–2112, 1987.
- Hooper SL, O'Neil MB, Wagner R, Ewer J, Golowasch J, Marder E.** The innervation of the pyloric region of the crab, *Cancer borealis*: homologous muscles in decapod species are differently innervated. *J Comp Physiol A* 159: 227–240, 1986.
- Hua VB, Chang AB, Tchieu JH, Kumar NM, Nielsen PA, Saier MH, Jr.** Sequence and phylogenetic analyses of 4 TMS junctional proteins of animals: connexins, innexins, claudins and occludins. *J Membr Biol* 194: 59–76, 2003.
- Johnson BR, Peck JH, Harris-Warrick RM.** Amine modulation of electrical coupling in the pyloric network of the lobster stomatogastric ganglion. *J Comp Physiol A* 172: 715–732, 1993a.
- Johnson BR, Peck JH, Harris-Warrick RM.** Dopamine induces sign reversal at mixed chemical-electrical synapses. *Brain Res* 625: 159–164, 1993b.
- Johnson BR, Peck JH, Harris-Warrick RM.** Differential modulation of chemical and electrical components of mixed synapses in the lobster stomatogastric ganglion. *J Comp Physiol A* 175: 233–249, 1994.
- Kandarian B, Sethi J, Wu A, Baker M, Yazdani N, Kym E, Sanchez A, Edsall L, Gaasterland T, Macagno E.** The medicinal leech genome encodes 21 innexin genes: different combinations are expressed by identified central neurons. *Dev Genes Evol* 222: 29–44, 2012.
- Kepler TB, Marder E, Abbott LF.** The effect of electrical coupling on the frequency of model neuronal oscillators. *Science* 248: 83–85, 1990.
- Kothmann WW, Massey SC, O'Brien J.** Dopamine-stimulated dephosphorylation of connexin 36 mediates All amacrine cell uncoupling. *J Neurosci* 29: 14903–14911, 2009.
- Landisman CE, Connors BW.** Long-term modulation of electrical synapses in the mammalian thalamus. *Science* 310: 1809–1813, 2005.
- Landisman CE, Long MA, Beierlein M, Deans MR, Paul DL, Connors BW.** Electrical synapses in the thalamic reticular nucleus. *J Neurosci* 22: 1002–1009, 2002.
- Lasater EM, Dowling JE.** Dopamine decreases conductance of the electrical junctions between cultured retinal horizontal cells. *Proc Natl Acad Sci USA* 82: 3025–3029, 1985.
- Lewis TJ, Rinzel J.** Self-organized synchronous oscillations in a network of excitable cells coupled by gap junctions. *Network* 11: 299–320, 2000.
- Marder E.** Electrical synapses: rectification demystified. *Curr Biol* 19: R34–R35, 2009.
- Nadarajah B, Jones AM, Evans WH, Parnavelas JG.** Differential expression of connexins during neocortical development and neuronal circuit formation. *J Neurosci* 17: 3096–3111, 1997.
- Nagy JI, Bautista W, Blakley B, Rash JE.** Morphologically mixed chemical-electrical synapses formed by primary afferents in rodent vestibular nuclei as revealed by immunofluorescence detection of connexin36 and vesicular glutamate transporter-1. *Neuroscience* 252: 468–488, 2013.
- Nagy JI, Dudek FE, Rash JE.** Update on connexins and gap junctions in neurons and glia in the mammalian nervous system. *Brain Res Brain Res Rev* 47: 191–215, 2004.
- O'Brien J.** The ever-changing electrical synapse. *Curr Opin Neurobiol* 29C: 64–72, 2014.
- Panchin Y, Kelmans I, Matz M, Lukyanov K, Usman N, Lukyanov S.** A ubiquitous family of putative gap junction molecules. *Curr Biol* 10: R473–R474, 2000.
- Pereda AE, Curti S, Hoge G, Cachope R, Flores CE, Rash JE.** Gap junction-mediated electrical transmission: regulatory mechanisms and plasticity. *Biochim Biophys Acta* 1828: 134–146, 2013.
- Pfeuty B, Mato G, Golomb D, Hansel D.** Electrical synapses and synchrony: the role of intrinsic currents. *J Neurosci* 23: 6280–6294, 2003.
- Phelan P, Bacon JP, Davies JA, Stebbings LA, Todman MG, Avery L, Baines RA, Barnes TM, Ford C, Hekimi S, Lee R, Shaw JE, Starich TA, Curtin KD, Sun YA, Wyman RJ.** Innexins: a family of invertebrate gap-junction proteins. *Trends Genet* 14: 348–349, 1998.
- Phelan P, Goulding LA, Tam JL, Allen MJ, Dawber RJ, Davies JA, Bacon JP.** Molecular mechanism of rectification at identified electrical synapses in the *Drosophila* giant fiber system. *Curr Biol* 18: 1955–1960, 2008.
- Phelan P, Starich TA.** Innexins get into the gap. *Bioessays* 23: 388–396, 2001.
- Ransdell JL, Faust TB, Schulz DJ.** Correlated levels of mRNA and soma size in single identified neurons: evidence for compartment-specific regulation of gene expression. *Front Mol Neurosci* 3: 116, 2010.
- Rash JE, Curti S, Vanderpool KG, Kamasawa N, Nannapaneni S, Palacios-Prado N, Flores CE, Yasumura T, O'Brien J, Lynn BD, Bukauskas FF, Nagy JI, Pereda AE.** Molecular and functional asymmetry at a vertebrate electrical synapse. *Neuron* 79: 957–969, 2013.
- Rash JE, Dillman RK, Bilhartz BL, Duffy HS, Whalen LR, Yasumura T.** Mixed synapses discovered and mapped throughout mammalian spinal cord. *Proc Natl Acad Sci USA* 93: 4235–4239, 1996.
- Rela L, Szczupak L.** In situ characterization of a rectifying electrical junction. *J Neurophysiol* 97: 1405–1412, 2007.
- Saez JC, Connor JA, Spray DC, Bennett MV.** Hepatocyte gap junctions are permeable to the second messenger, inositol 1,4,5-trisphosphate, and to calcium ions. *Proc Natl Acad Sci USA* 86: 2708–2712, 1989.
- Sasaki K, Cropper EC, Weiss KR, Jing J.** Functional differentiation of a population of electrically coupled heterogeneous elements in a microcircuit. *J Neurosci* 33: 93–105, 2013.
- Schulz DJ, Goaillard JM, Marder E.** Variable channel expression in identified single and electrically coupled neurons in different animals. *Nat Neurosci* 9: 356–362, 2006.
- Schulz DJ, Goaillard JM, Marder EE.** Quantitative expression profiling of identified neurons reveals cell-specific constraints on highly variable levels of gene expression. *Proc Natl Acad Sci USA* 104: 13187–13191, 2007.
- Sherman A, Rinzel J.** Rhythrogenic effects of weak electrotonic coupling in neuronal models. *Proc Natl Acad Sci USA* 89: 2471–2474, 1992.
- Soto-Trevino C, Rabah P, Marder E, Nadim F.** Computational model of electrically coupled, intrinsically distinct pacemaker neurons. *J Neurophysiol* 94: 590–604, 2005.
- Spray DC, Ginzberg RD, Morales EA, Gatmaitan Z, Arias IM.** Electrophysiological properties of gap junctions between dissociated pairs of rat hepatocytes. *J Cell Biol* 103: 135–144, 1986.
- Spray DC, Harris AL, Bennett MV.** Voltage dependence of junctional conductance in early amphibian embryos. *Science* 204: 432–434, 1979.
- Starich T, Sheehan M, Jadrich J, Shaw J.** Innexins in *C. elegans*. *Cell Commun Adhes* 8: 311–314, 2001.
- Starich TA, Lee RY, Panzarella C, Avery L, Shaw JE.** eat-5 and unc-7 represent a multigene family in *Caenorhabditis elegans* involved in cell-cell coupling. *J Cell Biol* 134: 537–548, 1996.
- Starich TA, Xu J, Skerrett IM, Nicholson BJ, Shaw JE.** Interactions between innexins UNC-7 and UNC-9 mediate electrical synapse specificity in the *Caenorhabditis elegans* locomotory nervous system. *Neural Dev* 4: 16, 2009.
- Stebbins LA, Todman MG, Phillips R, Greer CE, Tam J, Phelan P, Jacobs K, Bacon JP, Davies JA.** Gap junctions in *Drosophila*: developmental expression of the entire innexin gene family. *Mech Dev* 113: 197–205, 2002.
- Temporal S, Lett KM, Schulz DJ.** Activity-dependent feedback regulates correlated ion channel mRNA levels in single identified motor neurons. *Curr Biol* 24: 1899–1904, 2014.
- Tobin AE, Cruz-Bermudez ND, Marder E, Schulz DJ.** Correlations in ion channel mRNA in rhythmically active neurons. *PLoS One* 4: e6742, 2009.
- Traub RD, Kopell N, Bibbig A, Buhl EH, LeBeau FE, Whittington MA.** Gap junctions between interneuron dendrites can enhance synchrony of gamma oscillations in distributed networks. *J Neurosci* 21: 9478–9486, 2001.
- Veruki ML, Hartveit E.** Electrical synapses mediate signal transmission in the rod pathway of the mammalian retina. *J Neurosci* 22: 10558–10566, 2002.

- Vervaeke K, Lorincz A, Gleeson P, Farinella M, Nusser Z, Silver RA.** Rapid desynchronization of an electrically coupled interneuron network with sparse excitatory synaptic input. *Neuron* 67: 435–451, 2010.
- Weaver AL, Roffman RC, Norris BJ, Calabrese RL.** A role for compromise: synaptic inhibition and electrical coupling interact to control phasing in the leech heartbeat CpG. *Front Behav Neurosci* 4: 2010.
- Weimann JM, Marder E.** Switching neurons are integral members of multiple oscillatory networks. *Curr Biol* 4: 896–902, 1994.
- Weimann JM, Meyrand P, Marder E.** Neurons that form multiple pattern generators: identification and multiple activity patterns of gastric/pyloric neurons in the crab stomatogastric system. *J Neurophysiol* 65: 111–122, 1991.
- White JG, Southgate E, Thomson JN, Brenner S.** The structure of the nervous system of the nematode *Caenorhabditis elegans*. *Philos Trans R Soc Lond B Biol Sci* 314: 1–340, 1986.
- Wu CL, Shih MF, Lai JS, Yang HT, Turner GC, Chen L, Chiang AS.** Heterotypic gap junctions between two neurons in the *Drosophila* brain are critical for memory. *Curr Biol* 21: 848–854, 2011.
- Yen MR, Saier MH, Jr.** Gap junctional proteins of animals: the innixin/pannexin superfamily. *Prog Biophys Mol Biol* 94: 5–14, 2007.

